

Article

Controlling Polymer Composition in Organocatalyzed Photoredox Radical Ring-Opening Polymerization of Vinylcyclopropanes

Dian-Feng Chen, Bret Boyle, Blaine McCarthy, Chern-Hooi Lim, and Garret M. Miyake

J. Am. Chem. Soc., **Just Accepted Manuscript** • Publication Date (Web): 29 Jul 2019

Downloaded from pubs.acs.org on July 29, 2019

Just Accepted

"Just Accepted" manuscripts have been peer-reviewed and accepted for publication. They are posted online prior to technical editing, formatting for publication and author proofing. The American Chemical Society provides "Just Accepted" as a service to the research community to expedite the dissemination of scientific material as soon as possible after acceptance. "Just Accepted" manuscripts appear in full in PDF format accompanied by an HTML abstract. "Just Accepted" manuscripts have been fully peer reviewed, but should not be considered the official version of record. They are citable by the Digital Object Identifier (DOI®). "Just Accepted" is an optional service offered to authors. Therefore, the "Just Accepted" Web site may not include all articles that will be published in the journal. After a manuscript is technically edited and formatted, it will be removed from the "Just Accepted" Web site and published as an ASAP article. Note that technical editing may introduce minor changes to the manuscript text and/or graphics which could affect content, and all legal disclaimers and ethical guidelines that apply to the journal pertain. ACS cannot be held responsible for errors or consequences arising from the use of information contained in these "Just Accepted" manuscripts.

Controlling Polymer Composition in Organocatalyzed Photoredox Radical Ring-Opening Polymerization of Vinylcyclopropanes

Dian-Feng Chen, Bret M. Boyle, Blaine G. McCarthy, Chern-Hooi Lim, and Garret M. Miyake*

Department of Chemistry, Colorado State University, Fort Collins, CO 80523, United States

ABSTRACT

Although radical polymerizations are among the most prevalent methodologies for the synthesis of polymers with diverse compositions and properties, the intrinsic reactivity and selectivity of radical addition challenges the ability to impart control over the polymerization propagation and produce polymers with defined microstructure. Vinylcyclopropanes (VCPs) can be polymerized through radical ring-opening polymerization to produce polymers possessing linear (*l*) or cyclic (*c*) repeat units providing opportunity to control polymer structure and modify the polymer properties. Herein, we report the first organocatalyzed photoredox radical ring-opening polymerization of a variety of functionalized VCP monomers, where high monomer conversions and spatial and temporal control were achieved to produce poly(VCPs) with predictable molecular weight and low dispersity. Through manipulating polymerization concentration and temperature, tunable *l* or *c* content was realized, allowing further investigation of thermal and viscoelastic materials properties associated with these two distinct compositions. Unexpectedly, the photoredox catalysis enables a post-polymerization modification that converts *l* content into the *c* content. Combined experimental and computational studies suggested an intramolecular radical cyclization pathway, where cyclopentane and cyclohexane repeat units are likely formed.

INTRODUCTION

The merger of photoredox catalysis¹ and controlled polymerizations² have drawn increasing attention as to provide spatial and temporal control over the chain growth and produce polymers with predictable composition, molecular weight (MW), and low dispersity (\mathcal{D}) under mild conditions.³ A variety of methodologies which implement light to affect diverse reaction mechanisms have been discovered, including photoinduced atom transfer radical polymerization (ATRP),⁴ photoinduced electron/energy transfer reversible addition-fragmentation chain transfer polymerization,⁵ photocontrolled cationic polymerization,⁶ metal-free ring-opening metathesis polymerization,⁷ and others.⁸ Our interest in photoredox-controlled polymerization originated with the motivation to develop an organocatalyzed ATRP (O-ATRP). Our group and others have employed highly reducing organic photoredox catalysts (PCs), such as perylene,^{3e} phenothiazines,^{3f} *N,N*-diaryl dihydrophenazines³ⁱ and *N*-aryl phenoxazines,^{3j,9} for O-ATRP. To further advance this nascent polymerization methodology we are motivated to discover new reactivity of these organic photosystems that are otherwise inaccessible.

Vinylcyclopropanes (VCPs) are an intriguing class of monomers in that they can be polymerized through various pathways to yield drastically different polymeric structures, exhibiting low volume shrinkage or even volume expansion—a unique property of modeling and restorative materials.¹⁰ In a radical pathway, the radical ring-opening polymerization (rROP) proceeds to yield a polymer possessing a combination of unsaturated linear (*l*) and saturated cyclic (*c*) repeat units.¹¹ These *c* repeat units have been proposed to be cyclobutanes generated through a 4-*endo-trig* radical cyclization (Figure 1A).¹² To evaluate *l/c* selectivity, a linear factor S_L is defined here as the total percentage of *l* repeat units. Most rROP approaches have utilized traditional free radical polymerization techniques, which achieve low selectivity between *l* or *c* content and produce polymers with ill-defined MW characteristics (Figure 1B).¹² To address this limitation, Cu-ATRP was attempted for the rROP (ATrROP) of 1,1-diethoxycarbonyl-2-vinylcyclopropane (EtVCP) to produce well-defined polymers possessing a high *l* content ($S_L = 98\%$).¹³ However, presumable bidentate coordination from EtVCP or poly(EtVCP) to the Cu(I) catalyst inhibits polymerization to reach high monomer conversions (<50%)¹⁴ even at elevated temperatures (Figure 1C). Leveraging our recent advances in O-ATRP,

we envisaged that the use of an organic PC could eliminate this unfavorable coordination,¹⁵ enabling high monomer conversion and *l/c* selectivity while affording spatial and temporal control over the chain growth.

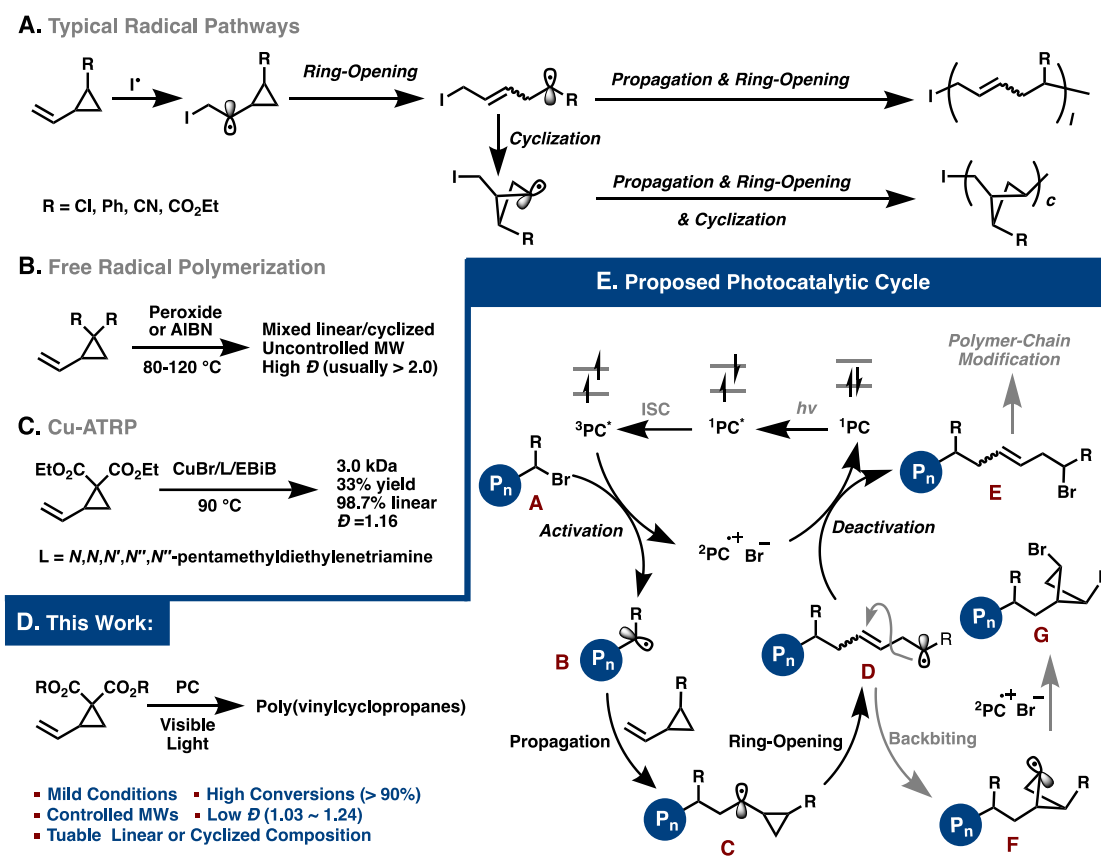


Figure 1. Profile of radical ring-opening polymerizations of 1,1-disubstituted vinylcyclopropanes.

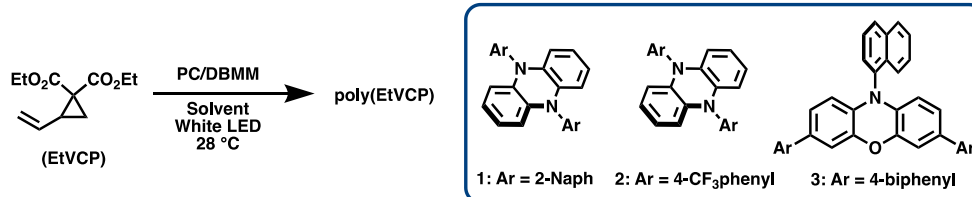
Herein, we demonstrate a photoredox-controlled approach utilizing *N,N*-diaryl dihydrophenazine PCs to address the challenges of polymerization efficiency and *l/c* selectivity (Figure 1D). Given their strong excited-state reduction potentials these organic PCs are able to activate the dormant alkyl bromide polymer chain (Figure 1E, A) to generate a propagating radical B. After monomer additions, recapping of the homoallylic radical intermediate D generated from the ring-opening of C by the $[^2\text{PC}^{*+}][\text{Br}^-]$ complex results in the dormant polymer E. Previously proposed backbiting cyclization of D may occur to form *c* repeat units. To mitigate side-reactivity, low loading of the PC may minimize radical concentrations in solution and minimize bimolecular radical termination pathways. As such, in our system a series of well-defined poly(VCPs) were obtained with

controlled MWs, low \bar{D} , and predominately l repeat units (S_L up to 98%). Moreover, through manipulation of polymerization conditions including temperature and concentration, tunable l/c selectivity was achieved ($S_L = 1$ –98%), thus enabling investigation of the polymer properties associated with such distinct chemical compositions. Moreover, a photoredox polymer-chain modification converting l composition into c composition suggests that the cyclic repeat units in poly(VCPs) are likely a mixture of cyclopentanes, cyclohexanes, and previously proposed cyclobutanes.

RESULTS AND DISCUSSION

Synthesis of poly(EtVCP) with high l content. Initial polymerization studies employed EtVCP as the monomer, diethyl 2-bromo-2-methylmalonate (DBMM) as the initiator, and N,N -dimethylacetamide (DMAc) as the solvent to investigate the catalyst performance on the polymerizations using standard O-ATRP conditions of ([EtVCP]:[DBMM]:[PC] = [1000]:[10]:[1] with irradiation by white LEDs and a cooling fan to maintain polymerization temperature at $\sim 28^\circ\text{C}$). Three PCs, including N,N -diaryl dihydrophenazines **1**–**2**, and 3,7-di(4-biphenyl)- N -naphthylphenoxazine **3**, were found to be able to drive the polymerization and produced poly(EtVCP) with high l content ($S_L = 97\%$, Table 1, entries 1–3). Polymers synthesized using PCs **2** and **3** displayed superior control over polymer molecular weight, with a number average molecular weight (M_n) close to the theoretical values, as is indicated by initiator efficiencies ($I^* = M_{n,\text{theo}}/M_{n,\text{measured}} \times 100\%$) close to 100% (entries 2–3). Conversely, polymerization with PC **1** afforded lower $\bar{D} = 1.21$ (entry 1). In a comparison between common ATRP alkyl bromide initiators (Table S1), DBMM proved to be superior, with polymerization reaching the highest monomer conversion and producing polymers with low \bar{D} and high I^* . A screen of solvents (entries 4–6) revealed that EtOAc allowed for the best control over the polymerization, achieving 98% monomer conversion in 8 hours, producing poly(EtVCP) with $\bar{D} = 1.15$, high S_L of 97%, and predictable MW as evidenced by an I^* of 99% (entry 4). No monomer conversion was observed in the absence of light, PC, or initiator, providing evidence of a photoredox-controlled ATRP mechanism (Table S2).

Table 1. Optimization of the synthesis of poly(EtVCP) with high *l* content.^a



| Entry | PC | Solvent | [M]/[I]/[PC] | Conv. (%) ^b | <i>M</i> _n (kDa) ^c | <i>Đ</i> (<i>M</i> _w / <i>M</i> _n) ^c | <i>I</i> [*] (%) ^d | <i>S</i> _L (%) ^b |
|-------|----|---------------------------------|--------------|---------------------------|---------------------------------------------|----------------------------------------------------------------------------|-------------------------------------------|-------------------------------------------|
| 1 | 1 | DMAc | 1000/10/1 | 72 | 22.6 | 1.21 | 69 | 97 |
| 2 | 2 | DMAc | 1000/10/1 | 70 | 16.8 | 1.63 | 90 | 97 |
| 3 | 3 | DMAc | 1000/10/1 | 77 | 15.5 | 1.53 | 107 | 97 |
| 4 | 1 | EtOAc | 1000/10/1 | 98 | 21.1 | 1.15 | 99 | 97 |
| 5 | 1 | CH ₂ Cl ₂ | 1000/10/1 | 99 | 29.0 | 1.20 | 74 | 96 |
| 6 | 1 | PhCl | 1000/10/1 | 99 | 22.3 | 1.17 | 97 | 94 |
| 7 | 1 | EtOAc | 1000/10/2 | 93 | 20.4 | 1.24 | 98 | 97 |
| 8 | 1 | EtOAc | 1000/10/0.5 | 98 | 19.8 | 1.17 | 106 | 97 |
| 9 | 1 | EtOAc | 1000/10/0.1 | 94 | 20.1 | 1.29 | 99 | 92 |
| 10 | 1 | EtOAc | 1000/20/1 | 99 | 11.8 | 1.12 | 91 | 97 |
| 11 | 1 | EtOAc | 1000/5/1 | 99 | 41.7 | 1.21 | 101 | 97 |
| 12 | 1 | EtOAc | 500/10/1 | 98 | 11.6 | 1.10 | 92 | 97 |
| 13 | 1 | EtOAc | 2000/10/1 | 97 | 39.7 | 1.25 | 104 | 94 |
| 14 | 1 | EtOAc | 5000/10/1 | 95 | 79.5 | 1.43 | 127 | 90 |

^aPolymerizations performed using 1.0 mmol of EtVCP, DBMM as the initiator, 1.0 mL of solvent, and irradiated by white LEDs at 28 °C for 8 h. ^bMeasured by crude ¹H-NMR. $S_L = I/(I + c)$. ^cMeasured by GPC. ^dInitiator efficiency (I^*) = $M_{n,theo}/M_{n,measured} \times 100\%$, where $M_{n,theo} = MW(\text{initiator}) + MW(\text{EtVCP}) \times \text{conversion} \times ([\text{EtVCP}]/[\text{initiator}])$.

Using PC **1**, catalyst loadings could be decreased to 100 ppm while still maintaining polymerization control [$M_n = 20.1$ kDa, $\mathcal{D} = 1.29$, and $I^* = 99\%$, (entry 9)]. Further, modulation of the monomer or initiator stoichiometry allowed for synthesis of poly(EtVCP) with targeted MWs (from 11.8 to 79.5 kDa) and low to moderate dispersities ($\mathcal{D} = 1.10$ –1.43) (entries 10–14). First-order kinetics were observed for monomer conversion in the PC **1** catalyzed ATrROP of EtVCP at 28 °C (Figure 2A). Polymerization progress analysis revealed a linear increase in polymer MW as a function of monomer conversion, while low

dispersity ($\bar{D} = 1.17\text{--}1.22$) remained during the entire course of polymerization (Figure 2B).

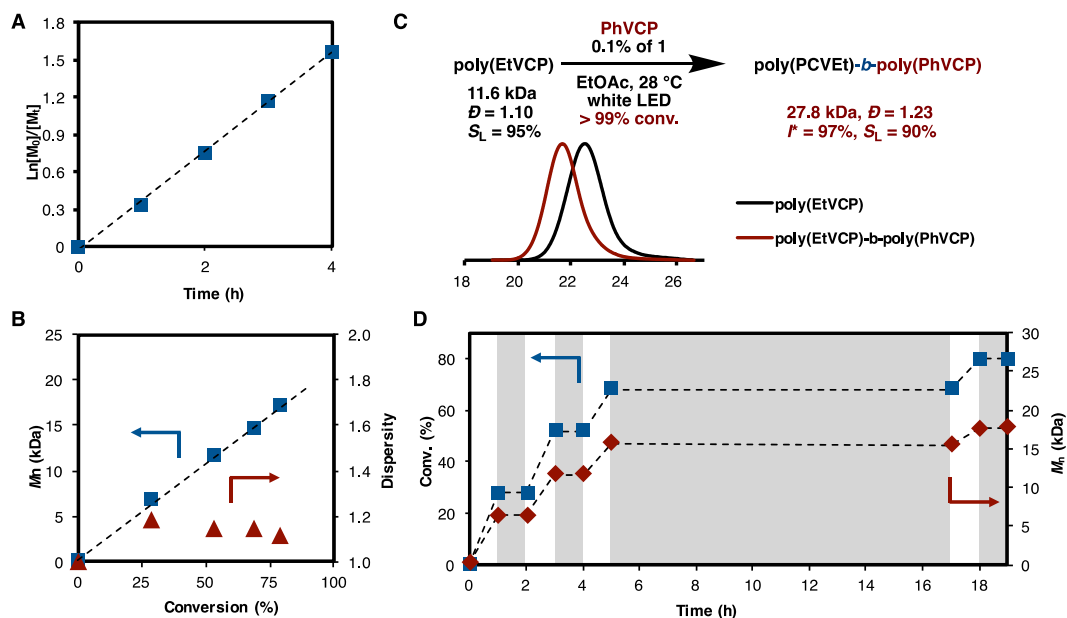


Figure 2. Synthesis of poly(EtVCP) with high l content: (A) Plots of the natural log of monomer conversion as a function of time. (B) Plots of experimentally measured M_n and dispersity as a function of monomer conversion. (C) Chain-extension polymerization from a poly(EtVCP) macroinitiator with PhVCP and GPC traces before and after polymerization. (D) Plots of monomer conversion and experimentally measured M_n as a function of time for a pulsed irradiation experiment.

To evaluate the control imparted by this photoredox organocatalyzed ATrROP (O-ATrROP), a series of experiments probing chain-end group fidelity were performed to analyze the reversible activation-deactivation equilibrium. First, matrix-assisted laser desorption ionization time of flight mass spectrum (MALDI-TOF MS) was performed (Figure S11). In accordance with the proposed reversible activation-deactivation mechanism, the polymer possessed predominately Br chain-end groups as well as minor H chain-end groups, likely due to termination events during the polymerization or loss of the Br chain-end group during the MALDI-TOF MS analysis. The presence of the bromide chain-end groups allows for application of the synthesized polymers to serve as macroinitiators in subsequent polymerizations to access polymers with more complex composition. Thus, poly(EtVCP) ($M_n = 11.6$ kDa, $\bar{D} = 1.10$, $S_L = 97\%$) was synthesized, isolated, and employed as a macroinitiator for rROP of a different monomer 1,1-

diphenyloxycarbonyl-2-vinylcyclopropane (PhVCP) to synthesize a poly(EtVCP)-*b*-poly(PhVCP) copolymer. The synthesis of this block copolymer was supported by a combination of NMR characterization (Figure S13) and a shift in the retention time of the gel-permeation chromatography (GPC) polymer trace due to an increase in polymer MW ($M_n = 27.8$ kDa, $\bar{D} = 1.23$) (Figure 2C). Moreover, the block copolymer synthesis achieved a high I^* of 97%, highlighting the Br chain-end group fidelity of the macroinitiator. We also demonstrated temporal control, a key feature of photoredox-catalyzed processes, using a pulsed-irradiation experiment, where the polymerization proceeded only under light irradiation, paused during dark periods (as long as 12 h), and could be resumed with continued irradiation, further supporting the light-driven, reversible activation-deactivation mechanism of O-ATrROP (Figure 2D).

Synthesis of poly(EtVCP) with high *c* content. With the synthesis of poly(EtVCP) with high *l* content successfully established, we desired to also selectively target high *c* content. In free radical polymerization of vinylcyclopropane monomers it has been shown that using solvents (compared to bulk polymerization) or increasing the polymerization temperature promotes intramolecular backbiting cyclization, leading to decreased *l* composition.¹⁶ Accordingly, we first investigated the concentration effect on this O-ATrROP of EtVCP at room temperature. Indeed, polymerizations at lower concentration produced polymers with more *c* content as indicated by decreased S_L (Table 2, entries 1–6). It is noteworthy that polymerizations at low concentrations (0.098–0.192 mol/L) still retained excellent control over the chain-growth as indicated by low \bar{D} (1.12–1.15) and high I^* (80–107%) (entries 4–6). The S_L dramatically decreased from 67% to 38% when the polymerization using a concentration of 0.192 mol/L was performed at 60 °C (entry 4 *vs* 7). Using high power blue LED (Figure S27b) instead of the white LEDs continued to promote the formation of *c* content ($S_L = 18\%$, entry 8). This result illuminates the crucial role of light intensity in photocontrolled polymerizations.¹⁷ PC **2** was proven to be superior to **1**, producing poly(EtVCP) with I^* of 99%, \bar{D} of 1.09 and S_L of 16% (entry 8 *vs* 9). Lowering the PC loading resulted in slightly higher \bar{D} and I^* (entries 10–12). Control experiments that omitted either light, PC **2**, or DBMM from the system led to no monomer conversion (Table S6). Moreover, good control of MW as achieved by manipulating the stoichiometry of

monomer to initiator, producing poly(EtVCP) with low \bar{D} of 1.03–1.16 and S_L of 13–16% (entries 13–15).

Table 2. Optimization and synthesis of poly(EtVCP) with high c content.^a

| Entry | PC | Conc. [mol/L] | T (°C) | [M]/[I]/[PC] | Conv. (%) ^b | M_n (kDa) ^c | \bar{D} (M_w/M_n) _{c} | I^* (%) ^d | S_L (%) ^b |
|-----------------|----|------------------|-----------|--------------|---------------------------|-----------------------------|---------------------------------------------------------|---------------------------|---------------------------|
| 1 | 1 | 1.429 | 28 | 1000/10/1 | 98 | 21.8 | 1.21 | 97 | 97 |
| 2 | 1 | 0.833 | 28 | 1000/10/1 | 98 | 21.1 | 1.15 | 99 | 97 |
| 3 | 1 | 0.455 | 28 | 1000/10/1 | 98 | 26.1 | 1.14 | 81 | 80 |
| 4 | 1 | 0.192 | 28 | 1000/10/1 | 95 | 25.3 | 1.12 | 80 | 67 |
| 5 | 1 | 0.122 | 28 | 1000/10/1 | 90 | 17.5 | 1.13 | 107 | 60 |
| 6 | 1 | 0.098 | 28 | 1000/10/1 | 88 | 18.6 | 1.15 | 102 | 55 |
| 7 | 1 | 0.192 | 60 | 1000/10/1 | 95 | 25.3 | 1.07 | 81 | 38 |
| 8 ^e | 1 | 0.192 | 60 | 1000/10/1 | 98 | 23.8 | 1.15 | 86 | 18 |
| 9 ^e | 2 | 0.192 | 60 | 1000/10/1 | 97 | 21.1 | 1.09 | 99 | 16 |
| 10 ^e | 2 | 0.192 | 60 | 1000/10/0.5 | 95 | 19.7 | 1.09 | 104 | 19 |
| 11 ^e | 2 | 0.192 | 60 | 1000/10/0.2 | 91 | 19.1 | 1.15 | 102 | 15 |
| 12 ^e | 2 | 0.192 | 60 | 1000/10/0.1 | 83 | 16.4 | 1.21 | 109 | 17 |
| 13 ^e | 2 | 0.192 | 60 | 1000/5/1 | 98 | 41.0 | 1.16 | 102 | 14 |
| 14 ^e | 2 | 0.192 | 60 | 1000/2/1 | 97 | 82.8 | 1.03 | 124 | 13 |
| 15 ^e | 2 | 0.192 | 60 | 1000/1/1 | 91 | 105.4 | 1.03 | 183 | 16 |

^aPolymerizations performed using 1.0 mmol of EtVCP, DBMM as the initiator, in EtOAc and irradiated with white LED for 12h. ^bMeasured by crude ¹H-NMR. $S_L = l/(l + c)$. ^cMeasured by GPC. ^dInitiator efficiency (I^*) = $M_{n(\text{theo})}/M_{n(\text{measured})}$, where $M_{n(\text{theo})} = \text{MW}(\text{initiator}) + \text{MW}(\text{EtVCP}) \times \text{conversion} \times ([\text{EtVCP}]/[\text{initiator}])$. ^e34 W blue LED was used.

Despite using diluted conditions, first-order kinetics (Figure 3A), a linear increase in polymer MW, and low to moderate \bar{D} with respect to monomer conversions (Figure 3B) were observed although MALDI-TOF MS analysis of a poly(EtVCP) sample (Figure S31) showed a relatively higher contribution of H chain-end groups. Temporal control was also achieved using a pulsed irradiation experiment at 60 °C with high power blue LED (Figure 3C). The polymer MWs before and after a dark period were similar to each other, while \bar{D} slightly increased after a complete “on-off” cycle (Figure D). Chain-extension experiment

using isolated poly(EtVCP) with high c content (22.9 kDa, $\bar{D} = 1.16$, $S_L = 15\%$) as the macroinitiator with EtVCP at 28 °C was then performed (Figure E). Although good control was obtained ($\bar{D} = 1.17$, $I^* = 112\%$), only 46% monomer conversion was observed after 12 h, which we attributed to less reactive variants of Br chain-end group presented in the macroinitiator. At elevated temperature intramolecular cyclization is greatly promoted during polymerization, leading to increased formation of alkyl radicals (e.g., **F** in Figure 1E), and subsequent deactivation to form new alkyl bromide chain-end groups (e.g., **G** in Figure 1E), which are reasonably more difficult than bromomalonate to reduce by *PC (Figure S36–S37 and Table S9).

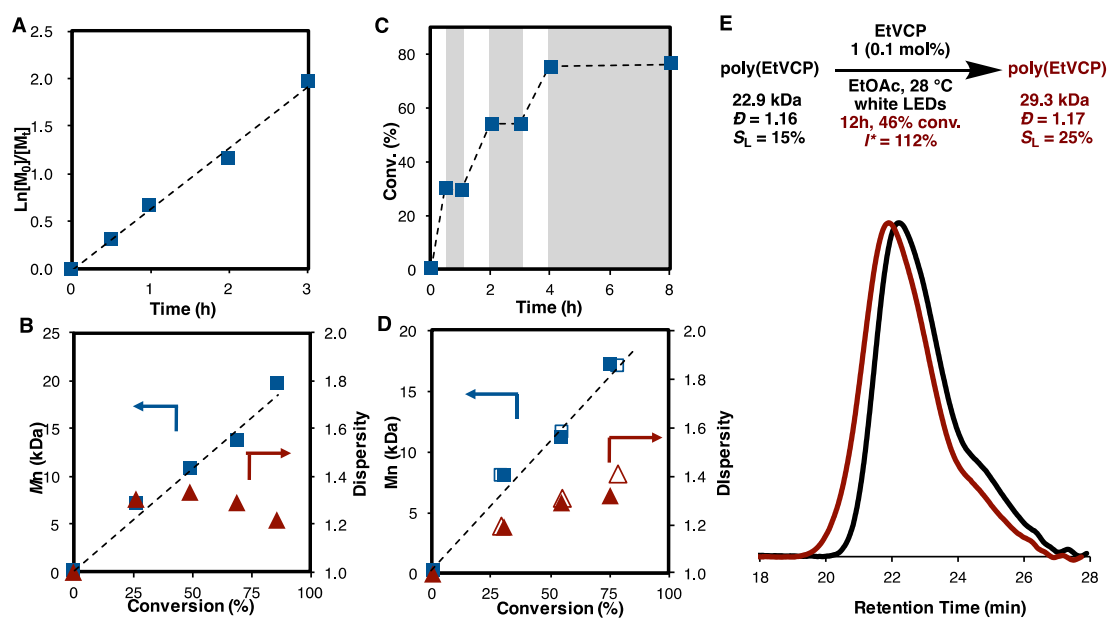
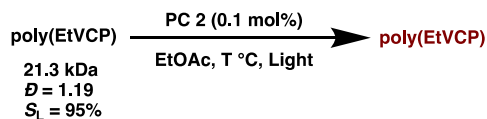


Figure 3. Synthesis of poly(EtVCP) with high c content: (A) Plots of the natural log of monomer conversion as a function of time. (B) Plots of experimentally measured M_n and \bar{D} as a function of monomer conversion. Plots of conversion versus time (C) and plots of M_n and \bar{D} as a function of monomer conversion (D) for pulsed irradiation experiment. Filled markers were data directly after irradiations, while open markers were data after the dark periods. (E) Chain-extension polymerization from a poly(EtVCP) macroinitiator with EtVCP and GPC traces before and after polymerization.

Post-polymerization modification of high l polymer-chain. Radical addition, such as thiol-ene “click” reaction,¹⁸ has been used to functionalize polymers containing internal C-C double bonds.¹⁹ The reactive alkene groups periodically spaced along the backbone

of poly(EtVCP) with high *l* content piqued our curiosity about the stability of this polymer-chain under photoredox conditions and the possibility to cross-link the resulting polymers. The investigation began with an isolated poly(EtVCP) (21.3 kDa, \bar{D} = 1.19, S_L = 95%), PC **2** (0.1 mol%), and white LEDs in EtOAc at 28 °C (Table 3, entries 1–2). Interestingly, reactions at 0.833 and 0.192 mol/L yielded soluble polymeric products with slightly decreased S_L values (90% and 86%, respectively) after 12 h, suggesting that transformation of the alkene groups in the polymer-chain indeed occurred, albeit not through significant cross-linking. Temperature also impacted this transformation such that S_L decreased from 95% to 80% after 12 h at 60 °C (entry 3). Surprisingly, replacing the light source with high power blue LED drastically promoted the conversion of *l* content into *c* content (S_L = 34%, entry 4). The increase in polymer MW (M_n = 35.2 kDa) when using the blue LED is likely due to radical-radical coupling terminations.

Table 3. Post-polymerization modification of poly(EtVCP) with high *l* content^a



| Entry | Conc. [mol/L] | T (°C) | M_n (kDa) ^b | \bar{D} (M_w/M_n) ^b | S_L (%) ^c |
|----------------|------------------|-----------|-----------------------------|-----------------------------------------|---------------------------|
| 1 | 0.833 | 28 | 23.8 | 1.22 | 90 |
| 2 | 0.192 | 28 | 24.3 | 1.23 | 86 |
| 3 | 0.192 | 60 | 27.6 | 1.15 | 80 |
| 4 ^e | 0.192 | 60 | 35.2 | 1.17 | 34 |

^aReactions performed using 1.0 mmol of poly(EtVCP) (21.3 kDa, \bar{D} = 1.09, S_L = 95%), in EtOAc and irradiated with white LED for 12h. The polymer was recovered quantitatively. ^bMeasured by GPC. ^cMeasured by crude ¹H-NMR. ^e34 W blue LED was used.

The resulted poly(EtVCP) from polymer-chain modification (Table 3, entry 4) exhibited excellent solubility in common organic solvents (e.g., EtOAc, ether, toluene, and dichloromethane). As such, we believe it is the intramolecular radical cyclization, other than polymer crosslinking, that contributes to the decrease of S_L . Due to difficult structural analysis based on NMR spectra,¹² we designed a model reaction to mimic the radical

cyclization and probe the mechanism. Three-step allylation of diethyl malonate afforded a compound **4** as a 6:1 *E/Z* mixture at C8 position, which was then placed under similar polymer-chain modification conditions (Figure 4). After 12 h, about 90% of starting material was recovered, and *E/Z* isomerization at the C3 position (**4'**) was observed (*E/Z* = 5.2:1). We attributed this C-C double bond isomerization to a reversible cyclization/fast ring-opening process, involving two potential pathways forming either cyclopropane or cyclobutane. Moreover, the cyclization product(s) **5** was also observed (in 5% isolated yield), which was likely a mixture of several cyclic bromides formed from distinct tandem cyclization pathways (two of the potential products are outlined in Figure 4; also see Figure S48–S51).

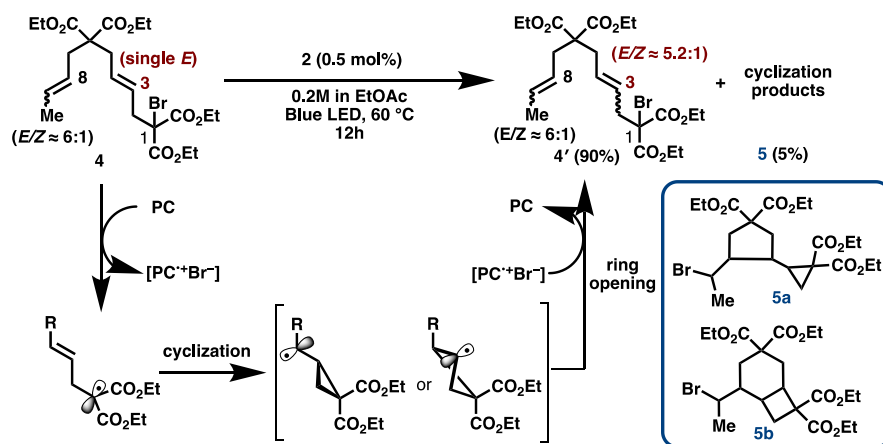


Figure 4. Results of model reaction of **4**.

However, for each tandem cyclization pathway, the resulting product consists of up to 8 diastereomers, which plagued the structural analysis of **5** and identification of cyclization mechanism. As such, we turned to density functional theory (DFT) calculations to predict cyclization pathways of a radical intermediate **6**, which is generated from two monomer additions of the initiator DBMM (Figure 5). Although *4-endo-trig* and *3-exo-trig* cyclizations of **6** are both endergonic (by 12.9 kcal and 2.7 kcal/mol, respectively), the latter is more favorable by 10.2 kcal/mol, which matches the classic Baldwin's rule.²⁰ The subsequent *5-exo-trig* and *6-endo-trig* cyclization pathways are both thermodynamically exergonic by more than 10 kcal/mol ($\Delta G = -11.8$ and -14.0 kcal/mol, respectively), indicating cyclopentane and cyclohexane are likely the favorable repeat units of chain-

modified poly(EtVCP). Moreover, cycloheptane may be accessible as well in this radical cyclization (Figure S52).

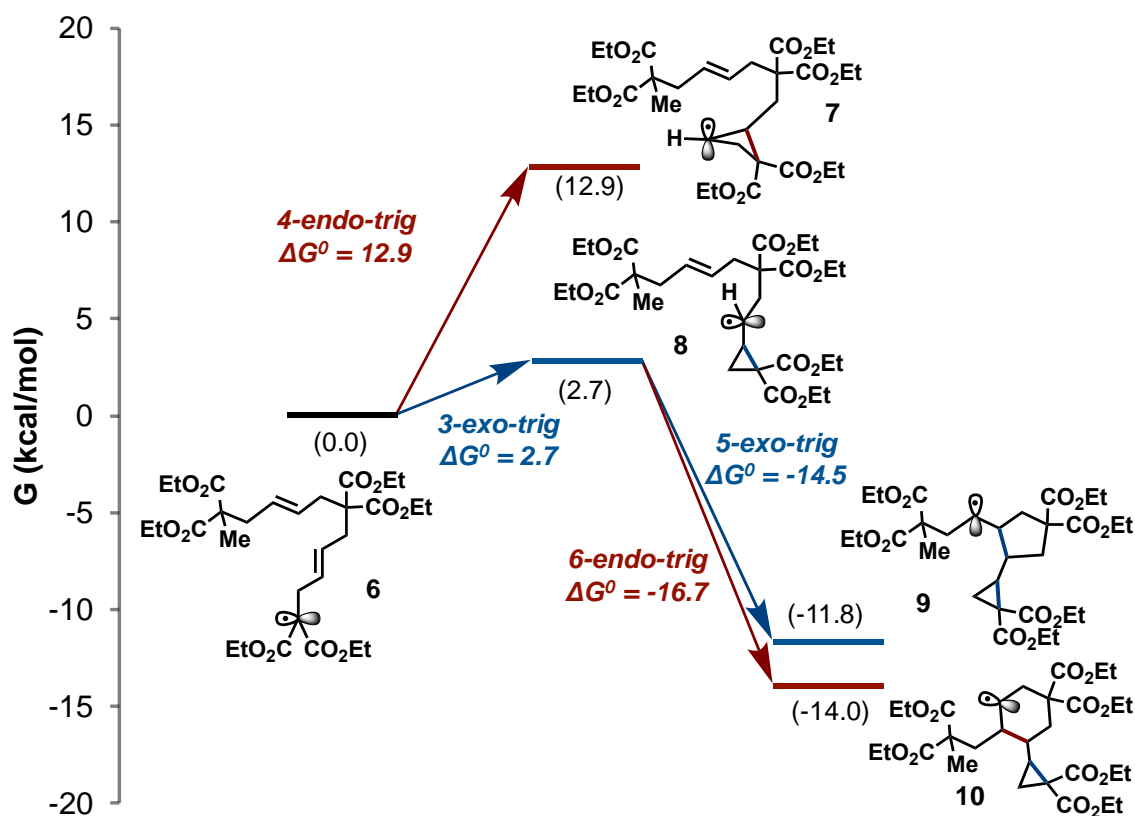


Figure 5. DFT calculations to predict late-stage cyclization pathways.

Mechanism for the formation of *c* content. In monitoring the polymerization performed at 60 °C (Figure 3A), we found that the S_L decreased over time (Table S7). This implies that considerable intramolecular cyclization is competing with propagation during polymerization at high temperature (60 °C). The *c* content is either from immediate backbiting (Figure 1E, from intermediate **D** to **F**) after the ring-opening process (Figure 1E, from intermediate **C** to **D**), or from tandem radical cyclization of an unsaturated linear polymer-chain of random length. To gain further insights into the chemical structures of *c* repeat units, comparison of the proton and carbon NMR spectra of three poly(EtVCP) samples synthesized from distinct methods, benzoyl peroxide (BPO) initiated bulk radical polymerization ($M_n = 25.1$ kDa, $\bar{D} = 3.8$, $S_L = 30\%$), photoredox ATRP of 0.192 mol/L with white LEDs at 60 °C ($M_n = 21.1$ kDa, $\bar{D} = 1.23$, $S_L = 40\%$), and polymer-chain

modification ($M_n = 35.2$ kDa, $\bar{D} = 1.17$, $S_L = 34\%$, Table 3, entry 4), was performed. These spectra are extremely similar (Figure S41–S43), suggesting that the aforementioned radical polymerizations (or modification) produce similar c composition, which are likely cyclobutanes, cyclopentanes, and cyclohexanes.

Characterizations of poly(EtVCP) with variable l or c content. To elucidate the differences that the degree of l or c content has on the polymer's behavior, the thermal and viscoelastic properties were investigated for four polymer samples of comparable MW (21–23 kDa) with S_L values ranging from 95 % to 15 % (Figure 6). Polymer **I**, with an S_L value of 95 %, has a glass transition temperature (T_g) of 32.6 °C, as shown by differential scanning calorimetry (DSC) (Figure 6B). As the S_L value decreases from 70 % in polymer **II**, to 35 % in polymer **III**, to 15 % in polymer **IV**, the T_g of the polymer samples also decrease from 31.2 °C to 30.8 °C to 28.5 °C, respectively. Therefore, as the c content increases, the side-chain free volume seems to increase. Further, the melting peaks associated with all four of the polymer samples become less apparent with increasing c content.

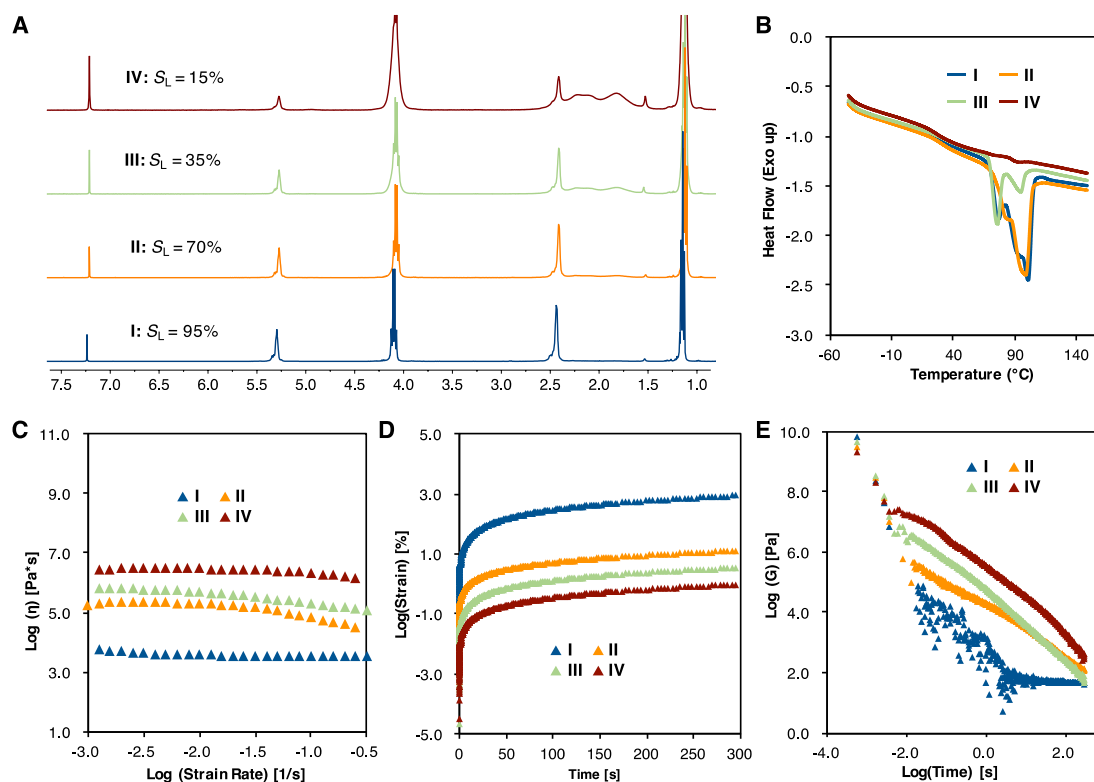
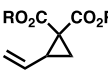
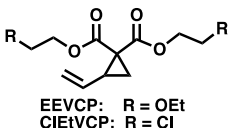
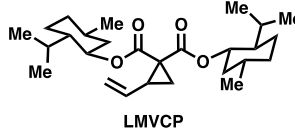


Figure 6. Comparison of ^1H -NMR spectra (A), DSC curves (B), viscosity flow curves (C), creep tests (D) and 5% step-strain stress relaxation plots (E) of four poly(EtVCP) samples: **(I)** 21.3 kDa, $\bar{D} = 1.19$, $S_L = 95\%$; **(II)** 21.1 kDa, $\bar{D} = 1.17$, $S_L = 70\%$; **(III)** 22.3 kDa, $\bar{D} = 1.18$, $S_L = 35\%$; **(IV)** 22.9 kDa, $\bar{D} = 1.17$, $S_L = 15\%$.

To investigate the effect that l content of the polymer has on the viscoelastic properties, a series of tests were completed on each polymer sample in the melt at isofrictional conditions ($T_g + 30\text{ }^\circ\text{C}$) which included a flow test with a strain rate sweep from 0.001 to 0.3 1/s, a creep test with a constant 100 Pa stress applied over 5 minutes, and a 5% step-strain stress relaxation experiment over 5 minutes (Figure 6C–6E). In each test performed, it was shown that the lower the S_L value, the more elastic the polymer behavior. For instance, polymer **I** has the lowest viscosity value ($5.58 \times 10^3 \text{ Pa}\cdot\text{s}$ at 0.001 1/s), is the most deformed during the creep tests ($8.47 \times 10^2 \%$), and relaxes the fastest after a 5 % step-strain (~ 5 seconds until a modulus value of 45 Pa was reached). In stark contrast, polymer **IV** has the highest viscosity value ($2.51 \times 10^6 \text{ Pa}\cdot\text{s}$ at 0.001 1/s), is the least deformed during the creep tests (0.929 %), and relaxes the slowest after a 5 % step-strain (300 seconds until a modulus value of 350 Pa was reached).

Table 4. Monomer Scope for Organocatalyzed rROP of Vinylcyclopanes^a

| <div style="display: flex; align-items: center; justify-content: space-around;"> <div style="text-align: center;">  </div> <div style="font-size: 0.8em;"> EtVCP: R = Et PrVCP: R = Pr BuVCP: R = Bu ^tBuVCP: R = ^tBu BnVCP: R = Bn PhVCP: R = Ph </div> <div style="text-align: center;">  </div> <div style="font-size: 0.8em;"> EEVCP: R = OEt ClEtVCP: R = Cl </div> <div style="text-align: center;">  </div> </div> | | | | | | | | | | |
|------------------------------------------------------------------------------------------------------------------------------------------------------------------------------------------------------------------------------------------------------------------------------------------------------------------------------------------------------------------------------------------------------------------------------------------------------------------------------------------------------------------------------------------------------------------------------------------------------------------------------------------------------------------------------------------------------------------------------------------------------------------------------------------------------------------------------------------------|--------------------|-----------|---------------------------|-----------------------------|-----------------------------------------|---------------------------|---------------------------|-------------------------------|-------------------------------|-------------------------------|
| Entry | Monomer | Condition | Conv. (%) ^b | M_n (kDa) ^c | \bar{D} (M_w/M_n) ^c | I^* (%) ^d | S_L (%) ^b | T_g ($^\circ\text{C}$) | T_m ($^\circ\text{C}$) | T_d ($^\circ\text{C}$) |
| 1 | EtVCP | A | 98 | 21.1 | 1.15 | 99 | 97 | 32 | 94 | 359 |
| 2 | EtVCP | B | 97 | 21.1 | 1.09 | 99 | 16 | 30 | - | 360 |
| 3 | PrVCP | A | 98 | 25.7 | 1.12 | 93 | 97 | 9 | 93 | 357 |
| 4 | PrVCP | B | 99 | 29.3 | 1.11 | 83 | 10 | 6 | - | 362 |
| 5 | BuVCP | A | 98 | 27.2 | 1.15 | 98 | 93 | -20 | 47 | 354 |
| 6 | BuVCP | B | 99 | 31.9 | 1.10 | 85 | 6 | -16 | - | 364 |
| 7 ^e | ^t BuVCP | A | 98 | 29.3 | 1.19 | 91 | 98 | 78 | 169 | 227 |

| | | | | | | | | | | |
|-----------------|--------------------------|---|----|------|------|-----|----|-----|-----|-----|
| 8 ^e | ^tBuVCP | B | 99 | 30.3 | 1.18 | 90 | 5 | 87 | - | 226 |
| 9 | BnVCP | A | 97 | 32.6 | 1.16 | 101 | 92 | 30 | 84 | 356 |
| 10 | BnVCP | B | 95 | 28.1 | 1.18 | 115 | 30 | 29 | - | 356 |
| 11 ^e | PhVCP | A | 97 | 30.9 | 1.24 | 98 | 95 | 81 | 183 | 369 |
| 12 ^e | PhVCP | B | 98 | 46.8 | 1.06 | 65 | 40 | 94 | 180 | 380 |
| 13 | EEVCP | A | 91 | 29.0 | 1.21 | 95 | 97 | -27 | - | 356 |
| 14 | EEVCP | B | 99 | 35.8 | 1.03 | 85 | 30 | -31 | - | 351 |
| 15 | CIEVCP | A | 93 | 26.9 | 1.23 | 98 | 92 | 47 | 179 | 342 |
| 16 | CIEVCP | B | 99 | 29.3 | 1.13 | 97 | 20 | 41 | - | 349 |
| 17 | LMVCP | A | 95 | 42.3 | 1.21 | 98 | 75 | 74 | 139 | 313 |
| 18 | LMVCP | B | 99 | 52.5 | 1.20 | 83 | 1 | 68 | - | 312 |

^a**Condition A:** [EtVCP]: [DBMM]: [1] = 1000 : 10 : 1, in 1.0 mL of EtOAc (0.833 mol/L), and with homemade white LED beaker at 28 °C for 8h. **Condition B:** [EtVCP]: [DBMM] : [1] = 1000 : 10 : 1, in 5.0 mL of EtOAc (0.192 mol/L), and with 34 W blue LED at 60 °C for 12h. ^bMeasured by crude ¹H-NMR. $S_L = l/(l + c)$. ^cMeasured by GPC. ^dInitiator efficiency (I^*) = $M_{n(\text{theo})}/M_{n(\text{measured})}$, where $M_{n(\text{theo})}$ = MW(initiator) + MW(EtVCP) × conversion × ([EtVCP]/[initiator]). ^ePhCl was used as the solvent.

Monomer scope. Subsequent exploration of the monomer scope revealed a variety of vinylcyclopropanes with diverse substituents being amenable to this organocatalyzed photoredox protocol (Table 4). Generally, polymerizations of 0.833 mol/L at 28 °C achieved high conversions (91–98%), near 100% I^* , low \bar{D} (1.12–1.24), and predominantly *l* contents (S_L = 92–98%). Low concentration (0.192 mol/L) polymerizations at 60 °C with high power blue LED were also high yielding (95–99% conversions), producing poly(vinylcyclopropanes) with low \bar{D} (1.06–1.20), moderate to excellent I^* (65–115%), and cyclic repeat units as the major composition (S_L = 5–40%). The glass transition temperature (T_g) of the resulting poly(vinylcyclopropanes) ranged from -31 to 94 °C, where additional methylene groups to the side chain might increase the free volume of the polymer, thereby significantly decreasing T_g . All of the obtained polymers exhibited decomposition temperatures (T_d) over 340 °C, except poly(^tBuVCP), which started to decompose at 227 °C (entries 7–8). Interestingly, the chemical compositions (*l* or *c* content) do not significantly impact the T_g and T_d , while most polymers exhibited melting points (T_m) ranging from 47 to 183 °C at high *l* content, and became amorphous at high *c* content.

Regardless of polymer compositions, no T_m was observed for poly(EEVCP) (entries 13–14).

CONCLUSION

In conclusion, we have established a general photoredox strategy for the radical ring-opening polymerizations of a series of functionalized vinylcyclopropane monomers, producing poly(vinylcyclopropanes) with predictable MW and low \bar{D} . The use of *N,N*-diaryl dihydrophenazines as the photocatalyst enables high monomer conversions (> 90%) under mild conditions. By manipulating polymerization concentration and temperature, unprecedented regulation on the linear and cyclic compositions of obtained polymers was achieved, which allowed investigations of composition-associated thermal and viscoelastic properties. Significantly, we have discovered a novel polymer-chain modification that converts *l* composition into *c* composition. The combination of a model reaction and DFT computations disclose several tandem radical cyclization pathways to produce cyclopentane and cyclohexane repeat units in the modified polymer. This post-polymerization modification also suggests a novel mechanism, besides previously proposed backbiting cyclization, to form the *c* composition during polymerization. Combined, these findings provide valuable insights to guide the future design and fabrication of poly(vinylcyclopropane)-based materials.

ASSOCIATED CONTENT

Supporting Information.

The Supporting Information is available free of charge on the ACS Publications website.

AUTHOR INFORMATION

Corresponding Author

*garret.miyake@colostate.edu

ORCID

Dian-Feng Chen: 0000-0003-1821-9783

Chern-Hooi Lim: 0000-0003-1823-6305

Garret M. Miyake: 0000-0003-2451-7090

Notes

The authors declare no competing financial interest.

ACKNOWLEDGMENT

This work was supported by Colorado State University, the Sloan Research Foundation, and the National Institute of General Medical Sciences of the National Institutes of Health under Award Number R35GM119702. The content is solely the responsibility of the authors and does not necessarily represent the official views of the National Institutes of Health. We acknowledge the use of computational resources provided by the XSEDE - Comet supercomputer (NSF ACI-1053575). C.-H.L. is grateful for an NIH F32 Postdoctoral Fellowship (F32GM122392). B.G.M. is grateful for support from an NSF GRFP. D.-F. C. thanks Bonnie L. Buss for technical assistance and helpful discussions.

REFERENCES

- ¹ (a) Narayanam, J. M. R.; Stephenson, C. R. J. Visible light photoredox catalysis: applications in organic synthesis. *Chem. Soc. Rev.* **2011**, *40*, 102–113. (b) Prier, C. K.; Rankic, D. A.; MacMillan, D. W. C. Visible light photoredox catalysis with transition metal complexes: applications in organic synthesis. *Chem. Rev.* **2013**, *113*, 5322–5363. (c) D. M. Schultz, T. P. Yoon, Solar Synthesis: Prospects in Visible Light Photocatalysis. *Science* **2014**, *343*, 1239176.
- ² Grubbs, R. B.; Grubbs, R. H. 50th anniversary perspective: living polymerization—emphasizing the molecule in macromolecules. *Macromolecules* **2017**, *50*, 6979–6997.
- ³ (a) Chen, M.; Zhong, M.; Johnson, J. A. Light-controlled radical polymerization: mechanisms, methods, and applications. *Chem. Rev.* **2016**, *116*, 10167–10211. (b) Corrigan, N.; Shanmugam, S.; Xu, J.; Boyer, C. Photocatalysis in organic and polymer synthesis. *Chem. Soc. Rev.* **2016**, *45*, 6165–6212. (c) McKenzie, T. G.; Fu, Q.; Uchiyama, M.; Satoh, K.; Xu, J.; Boyer, C.; Kamigaito, M.; Qiao, G. G. *Adv. Sci.* **2016**, *3*, 1500394. (d) Buss, B. L.; Miyake, G. M. Photoinduced controlled radical polymerizations performed in flow: methods, products, and opportunities. *Chem. Mater.* **2018**, *30*, 3931–3942. (e)

Discekici, E. H.; Anastasaki, A.; Read de Alaniz, J.; Hawker, C. J. Evolution and future directions of metal-free atom transfer radical polymerization. *Macromolecules* **2018**, *51*, 7421–7434.

⁴ For selected examples, see: (a) Fors, B. P.; Hawker, C. J. Control of a living radical polymerization of methacrylates by light. *Angew. Chem., Int. Ed.* **2012**, *51*, 8850–8853. (b) Mosnačėk, J.; Ilčíková, M. Photochemically mediated atom transfer radical polymerization of methyl methacrylate using ppm amounts of catalyst. *Macromolecules* **2012**, *45*, 5859–5865. (c) Konkolewicz, D.; Schroder, K.; Buback, J.; Bernhard, S.; Matyjaszewski, K. Visible light and sunlight photoinduced ATRP with ppm of Cu catalyst. *ACS Macro Lett.* **2012**, *1*, 1219–1223. (d) Anastasaki, A.; Nikolaou, V.; Zhang, Q.; Burns, J.; Samanta, S. R.; Waldron, C.; Haddleton, A. J.; McHale, R.; Fox, D.; Percec, V.; Wilson, P.; Haddleton, D. M. Copper(II)/tertiary amine synergy in photoinduced living radical polymerization: accelerated synthesis of ω -functional and α,ω -heterofunctional poly(acrylates). *J. Am. Chem. Soc.* **2014**, *136*, 1141–1149. (e) Miyake, G. M.; Theriot, J. C. Perylene as an organic photocatalyst for the radical polymerization of functionalized vinyl monomers through oxidative quenching with alkyl bromides and visible light. *Macromolecules* **2014**, *47*, 8255–8261. (f) Treat, N. J.; Sprafke, H.; Kramer, J. W.; Clark, P. G.; Barton, B. E.; Read de Alaniz, J.; Fors, B. P.; Hawker, C. J. Metal-free atom transfer radical polymerization. *J. Am. Chem. Soc.* **2014**, *136*, 16096–16101. (g) Pan, X.; Malhotra, N.; Simakova, A.; Wang, Z.; Konkolewicz, D.; Matyjaszewski, K. Photoinduced atom transfer radical polymerization with ppm-level Cu catalyst by visible light in aqueous media. *J. Am. Chem. Soc.* **2015**, *137*, 15430–15433. (h) Jones, G. R.; Whitfield, R.; Anastasaki, A.; Haddleton, D. M. Aqueous copper(II) photoinduced polymerization of acrylates: low copper concentration and the importance of sodium halide salts. *J. Am. Chem. Soc.* **2016**, *138*, 7346–7352. (i) Theriot, J. C.; Lim, C.-H.; Yang, H.; Ryan, M. D.; Musgrave, C. B.; Miyake, G. M. Organocatalyzed atom transfer radical polymerization driven by visible light. *Science* **2016**, *352*, 1082–1086. (j) Pearson, R. M.; Lim, C.-H.; McCarthy, B. G.; Musgrave, C. B.; Miyake, G. M. Organocatalyzed atom transfer radical polymerization using N-aryl phenoxazines as photoredox catalysts. *J. Am. Chem. Soc.* **2016**, *138*, 11399–11407. (k) Discekici, E. H.; Anastasaki, A.; Kaminker, R.; Willenbacher, J.; Truong, N. P.; Fleischmann, C.; Oschmann, B.; Lunn, D. J.; Read de Alaniz, J.; Davis, T. P.; Bates, C.

M.; Hawker, C. J. Light-mediated atom transfer radical polymerization of semi-fluorinated (meth)acrylates: facile access to functional materials. *J. Am. Chem. Soc.* 2017, **139**, 5939–5945.

⁵ For selected examples, see: (a) Xu, J.; Jung, K.; Atme, A., Shanmugam, S. & Boyer, C. A robust and versatile photoinduced living polymerization of conjugated and unconjugated monomers and its oxygen tolerance. *J. Am. Chem. Soc.* **2014**, *136*, 5508–5519. (b) Chen, M.; MacLeod, M. J.; Johnson, J. A. Visible-light-controlled living radical polymerization from a trithiocarbonate iniferter mediated by an organic photoredox catalyst. *ACS Macro Lett.* **2015**, *4*, 566–569. (c) Shanmugam, S.; Xu, J.; Boyer, C. Exploiting metalloporphyrins for selective living radical polymerization tunable over visible wavelengths. *J. Am. Chem. Soc.* **2015**, *137*, 9174–9185. (d) Shanmugam, S.; Boyer, C. Stereo-, temporal and chemical control through photoactivation of living radical polymerization: synthesis of block and gradient copolymers. *J. Am. Chem. Soc.* **2015**, *137*, 9988–9999. (e) Shanmugam, S.; Xu, J.; Boyer, C. Light-regulated polymerization under near-infrared/far-red irradiation catalyzed by Bacteriochlorophyll *a*. *Angew. Chem., Int. Ed.* **2016**, *55*, 1036–1040. (f) Xu, J.; Shanmugam, S.; Fu, C.; Aguey-Zinsou, K.-F.; Boyer, C. Selective photoactivation: from a single unit monomer insertion reaction to controlled polymer architectures. *J. Am. Chem. Soc.* **2016**, *138*, 3094–3106. (g) Chen, M.; Deng, S.; Gu, Y.; Lin, J.; MacLeod, M. J.; Johnson, J. A. Logic-controlled radical polymerization with heat and light: multiple-stimuli switching of polymer chain growth via a recyclable, thermally responsive, gel photoredox catalyst. *J. Am. Chem. Soc.* 2017, **139**, 2257–2266. (h) Chen, M. Gu, Y.; Singh, A.; Zhong, M.; Jordan, A. M.; Biswas, S.; Korley, L. T. J.; Balazs, A. C.; Johnson, J. A. Living additive manufacturing: transformation of parent gels into diversely functionalized daughter gels made possible by visible light photoredox catalysis. *ACS Cent. Sci.* **2017**, *3*, 124–134. (i) Gong, H.; Zhao, Y.; Shen, X.; Lin, J.; Chen, M. Organocatalyzed photo-controlled radical polymerization of semi-fluorinated (meth)acrylates driven by visible light. *Angew. Chem. Int. Ed.* **2018**, *57*, 333–337.

⁶ (a) Perkowski, A. J.; You, W.; Nicewicz, D. A. Visible Light Photoinitiated Metal-Free Living Cationic Polymerization of 4-Methoxystyrene. *J. Am. Chem. Soc.* **2015**, *137*, 7580–7583. (b) Messina, M. S.; Axtell, J. C.; Wang, Y.; Chong, P.; Wixtrom, A. I.; Kirlikovali, K. O.; Upton, B. M.; Hunter, B. M.; Shafaat, O. S.; Khan, S. I.; Winkler, J. R.; Gray, H.

B.; Alexandrova, A. N.; Maynard, H. D.; Spokoyny, A. M. Visible-light-induced olefin activation using 3D aromatic boron-rich cluster photooxidants. *J. Am. Chem. Soc.* **2016**, *138*, 6952–6955. (c) Kottisch, V.; Michaudel, Q.; Fors, B. P. Cationic Polymerization of Vinyl Ethers Controlled by Visible Light. *J. Am. Chem. Soc.* **2016**, *138*, 15535–15538. (d) Kottisch, V.; Michaudel, Q.; Fors, B. P. Photocontrolled interconversion of cationic and radical polymerizations. *J. Am. Chem. Soc.* **2017**, *139*, 10665–10668. (e) Michaudel, Q.; Chauviré, T.; Kottisch, V.; Supej, M. J.; Stawiasz, K. J.; Shen, L.; Zipfel, W. R.; Abruña, H. D.; Freed, J. H.; Fors, B. P. Mechanistic insight into the photocontrolled cationic polymerization of vinyl Ethers. *J. Am. Chem. Soc.* **2017**, *139*, 15530–15538.

⁷ (a) Ogawa, K. A.; Goetz, A. E.; Boydston, A. J. Metal-free ring-opening metathesis polymerization. *J. Am. Chem. Soc.* **2015**, *137*, 1400–1403. (b) Goetz, A. E.; Boydston, A. J. Metal-free preparation of linear and cross-linked polydicyclopentadiene. *J. Am. Chem. Soc.* **2015**, *137*, 7572–7575.

⁸ For selected examples, see: (a) Yamago, S.; Ukai, Y.; Matsumoto, A.; Nakamura, Y. Organotellurium-mediated controlled/living radical polymerization initiated by direct C–Te bond photolysis. *J. Am. Chem. Soc.* **2009**, *131*, 2100–2101. (b) Nakamura, Y.; Arima, T.; Tomita, S.; Yamago, S. Photoinduced switching from living radical polymerization to a radical coupling reaction mediated by organotellurium compounds. *J. Am. Chem. Soc.* **2012**, *134*, 5536–5539. (c) Ohtsuki, A.; Lei, L.; Tanishima, M.; Goto, A.; Kaji, H. Photocontrolled organocatalyzed living radical polymerization feasible over a wide range of wavelengths. *J. Am. Chem. Soc.* **2015**, *137*, 5610–5617.

⁹ McCarthy, B. G.; Pearson, R. M.; Lim, C.-H. Lim.; Sartor, S. M.; Damrauer, N. H.; Miyake, G. M. Structure–property relationships for tailoring phenoxazines as reducing photoredox catalysts. *J. Am. Chem. Soc.* **2018**, *140*, 5088–5101.

¹⁰ Moszner, N.; Zeuner, F.; Völkel, T.; Rheinberger, V. Synthesis and polymerization of vinylcyclopropanes. *Macromol. Chem. Phys.* **1999**, *200*, 2173–2187.

¹¹ Tardy, A.; Nicolas, J.; Gigmes, D.; Lefay, C.; Guillaneuf, Y. Radical ring-opening polymerization: scope, limitations, and application to (bio)degradable materials. *Chem. Rev.* **2017**, *117*, 1319–1406.

¹² Sanda, F.; Takata, T.; Endo, T. Radical polymerization behavior of 1,1-disubstituted 2-vinylcyclopropanes. *Macromolecules* **1993**, *26*, 1818–1824.

- ¹³ Singha, N. K.; Kavitha, A.; Sarker, P.; Rimmer, S. Copper-mediated controlled radical ring-opening polymerization (RROP) of a vinylcycloalkane. *Chem. Commun.* **2008**, 3049–3051.
- ¹⁴ (a) Lad, J.; Harrisson, S.; Mantovani, G.; Haddleton, D. M. Copper mediated living radical polymerisation: interactions between monomer and catalyst. *Dalton Trans.* **2003**, 4175–4180. (b) Mittal, A.; Sivaram, S.; Baskaran, D. Unfavorable coordination of copper with methyl vinyl ketone in atom transfer radical polymerization. *Macromolecules* **2006**, *39*, 5555–5558.
- ¹⁵ Lee, I.-H.; Discekici, E. H.; Anastasaki, A.; Read de Alaniz, J.; Hawker, C. J. Controlled radical polymerization of vinyl ketones using visible light. *Polym. Chem.* **2017**, *8*, 3351–3356.
- ¹⁶ Sugiyama, J.-I.; Ohashi, K.; Ueda, M. Free Radical Polymerization of Volume Expandable Vinylcyclopropane. *Macromolecules* **1994**, *27*, 5543–5546.
- ¹⁷ Ryan, M. D.; Pearson, R. M.; French, T. A.; Miyake, G. M. Impact of light intensity on control in photoinduced organocatalyzed atom transfer radical polymerization. *Macromolecules* **2017**, *50*, 4616–4622.
- ¹⁸ (a) Campos, L. M.; Killops, K. L.; Sakai, R.; Paulusse, J.-M. J.; Damiron, D.; Drockenmuller, E.; Messmore, B. W.; Hawker, C. J. Development of Thermal and Photochemical Strategies for Thiol-Ene Click Polymer Functionalization. *Macromolecules* **2008**, *41*, 7063–7070. (b) Lowe, A. B. Thiol-ene “click” reactions and recent applications in polymer and materials synthesis. *Polym. Chem.* **2010**, *1*, 17–36. (c) Lowe, A. B. Thiol-ene “click” reactions and recent applications in polymer and materials synthesis: a first update. *Polym. Chem.* **2014**, *5*, 4820–4870.
- ¹⁹ For selected examples, see: (a) Durmaz, H.; Butun, M.; Hizal, G.; Tunca, U. Postfunctionalization of polyoxanorbornene via sequential Michael addition and radical thiol-ene click reactions. *J. Polym. Sci., Part A: Polym. Chem.* **2012**, *50*, 3116–3125. (b) Van henberg, J. A.; Burford, R. P.; Lowe, A. B. Post-functionalization of a ROMP polymer backbone via radical thiol-ene coupling chemistry. *J. Polym. Sci., Part A: Polym. Chem.* **2013**, *51*, 487–492. (c) Walker, C. N.; Sarapas, J. M.; Kung, V.; Hall, A. L.; Tew, G. N. Multiblock copolymers by thiol addition across norbornene. *ACS Macro. Lett.* **2014**, *3*, 453–457. (d) Xiao, Z.; Bennett, C. W.; Connal, L. A. Facile and versatile platform for

the preparation of functional polyethylenes via thiol-ene chemistry. *J. Polym. Sci., Part A: Polym. Chem.* **2015**, 53, 1957–1960.

²⁰ Baldwin, J. E. Rules for ring closure. *J. Chem. Soc., Chem. Commun.*, **1976**, 734-736.

Table of Content image for

Controlling Polymer Composition in Organocatalyzed Photoredox Radical Ring-Opening Polymerization of Vinylcyclopropanes

Dian-Feng Chen, Bret M. Boyle, Blaine G. McCarthy, Chern-Hooi, Lim, and Garret M. Miyake*

Department of Chemistry, Colorado State University, Fort Collins, CO 80523, United States

